Phase Coexistence and Metal-Insulator Transition in Few-Layer Phosphorene: A Computational Study

Jie Guan, Zhen Zhu, and David Tománek[*]

Physics and Astronomy Department, Michigan State University, East Lansing, Michigan 48824, USA

Based on *ab initio* density functional calculations, we propose γ-P and δ-P as two additional stable structural phases of layered phosphorus besides the layered α-P (black) and β-P (blue) phosphorus allotropes. Monolayers of some of these allotropes have a wide band gap, whereas others, including γ-P, show a metal-insulator transition caused by in-layer strain or changing the number of layers. An unforeseen benefit is the possibility to connect different structural phases at no energy cost. This becomes particularly valuable in assembling heterostructures with well-defined metallic and semiconducting regions in one contiguous layer.

Layered black phosphorus is emerging as a viable contender in the competitive field of two-dimensional (2D) semiconductors [1,2]. In contrast to the popular semimetallic graphene, it displays a significant band gap while still maintaining a high carrier mobility [3–5]. The band gap in few-layer phosphorus, dubbed phosphorene, is believed to depend sensitively on the number of layers and in-layer strain [4,6–8]. Layered blue phosphorus, previously described as the $A7$ phase [9,10], has been predicted to be equally stable as black phosphorus but should have a different electronic structure [6]. It is intriguing to find out whether there are more than these two stable layered phosphorus allotropes and to what degree their dielectric response may be modified from a wide-gap semiconductor to a metal.

Here we introduce γ-P and δ-P as two additional stable structural phases of layered phosphorus besides the layered α-P (black) and β-P (blue) phosphorus allotropes. Based on our *ab initio* density functional calculations, we find these new structures, shown in Fig. 1, to be nearly as stable as the other layered allotropes. Monolayers of some of these allotropes have a wide band gap, whereas others, including γ-P, show a metal-insulator transition caused by in-layer strain or changing the number of layers. An unforeseen benefit is the possibility to connect different structural phases at no energy cost. This becomes particularly valuable in assembling heterostructures with well-defined metallic and semiconducting regions in one contiguous layer.

We utilize *ab initio* density functional theory (DFT) as implemented in the SIESTA [11] code to obtain insight into the equilibrium structure, stability, and electronic properties of γ-P and δ-P. We used periodic boundary conditions throughout the study, with multilayer structures represented by a periodic array of slabs separated by a 15 Å thick vacuum region. We used the Perdew-Burke-Ernzerhof (PBE) [12] exchange-correlation functional, norm-conserving Troullier-Martins pseudopotentials [13], and a double-ζ basis including

polarization orbitals. The reciprocal space was sampled by a fine grid [14] of $8 \times 8 \times 1$ k points in the Brillouin zone of the primitive unit cell or its equivalent in supercells. We used a mesh cutoff energy of 180 Ry to determine the self-consistent charge density, which provided us with a precision in total energy of $\lesssim 2$ meV/atom. All geometries have been optimized by using the conjugate gradient method [15], until none of the residual Hellmann-Feynman forces exceeded 10^{-2} eV/Å. Equilibrium structures and energies based on SIESTA were checked against values based on the VASP [16] code. We used VASP also to estimate the effect of van der Waals interactions, as implemented in the optimized exchange van der Waals functional B86b of Becke (optB86b vdW) functional [17,18], on the interlayer distances and interactions in the layered systems. For selected systems, we performed GW self-energy calculations using VASP.

Referring to the well-established black phosphorus structure as α-P and to blue phosphorus [6] as β-P, we present the optimized structure of these and two additional layered phosphorus allotropes, called γ-P and δ-P, in Fig. 1. All share the threefold coordination of all atoms and a nonzero intrinsic thickness of the layers, caused by the preference of phosphorus for a tetrahedral arrangement of its nearest neighbors. In fact, the differences among these structures arise from the different ways to connect tetrahedrally coordinated P atoms in a 2D lattice. There are four atoms in the rectangular Wigner-Seitz cell of γ-P and eight atoms in that of δ-P. The ridge structure of these phases is analogous to that of the anisotropic α-P but differs from the isotropic β-P with a hexagonal Wigner-Seitz cell containing only two atoms. The optimum structural parameters are summarized in Table I.

Results of our total energy calculations in Table I indicate that all layered structures are nearly equally stable, with cohesive energy differences below 0.1 eV. This comes as no surprise, since the local environment of the atoms is very similar, resulting in all bond lengths being close to
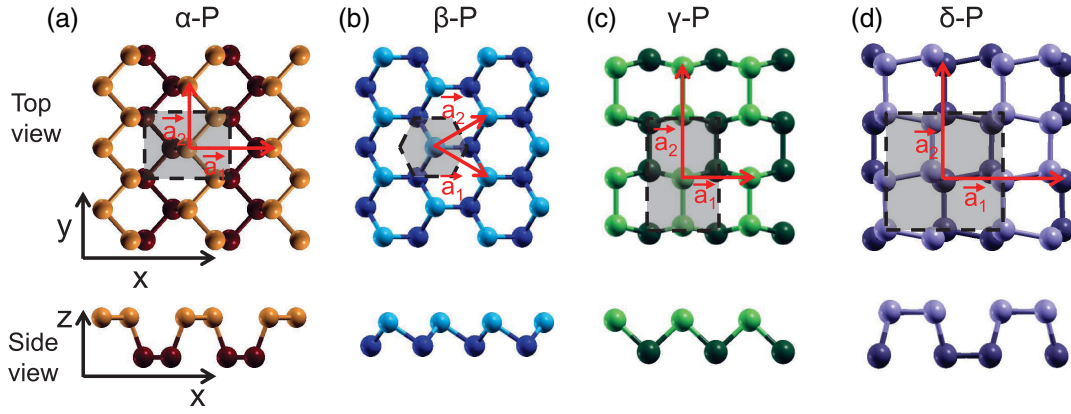
FIG. 1 (color online).   Equilibrium structure of (a) an α-P (black), (b) β-P (blue), (c) γ-P, and (d) δ-P monolayer in both top and side views. Atoms at the top and bottom of the nonplanar layers are distinguished by color and shading, and the Wigner-Seitz cells are shown by the shaded regions.

2.29 Å. We have verified the stability of the γ-P and δ-P phases by calculating their vibration spectra and by performing canonical molecular dynamics (MD) simulations. As seen in the Supplemental Material [22], the vibration spectra are free of soft modes associated with structural instabilities. Our MD results indicate that the two phases are not only stable at room temperature but do not spontaneously disintegrate even at $T = 1000$ K, slightly above the melting temperature $T_M = 863$ K of red phosphorus [21].

Our results for the optimum interlayer separation d ($d = |\vec{a_3}|$ for the AA layer stacking) and interlayer interaction energy E_{il} in the four phases are summarized in Table I. By not taking proper account of the van der Waals interactions [23,24], DFT-PBE calculations tend to underestimate E_{il} and overestimate d [4,6]. Probably the best, albeit computationally extremely demanding, way to correct this deficiency is the quantum Monte Carlo (QMC) approach [25]. QMC results for α-P indicate $E_{il} \approx 40$ meV/atom [26],

twice the 20 meV/atom value based on DFT-PBE, as cited in Table I. We also list the value obtained for α-P by using the van der Waals-corrected optB86b vdW functional, $E_{il} \approx 120$ meV/atom, which is significantly larger than the more trustable QMC value. Very similar corrections to the interlayer interaction of $\lesssim 0.1$ eV and a reduction of the interlayer distance are also obtained for the other layered allotropes. In spite of these minor differences, we find the interlayer interactions and distances to be rather similar in all these allotropes and in reasonable agreement with observed data in the only previously known black phosphorus (α-P) allotrope.

The calculated energy differences between the AA, AB, and ABC stacking of layers of a few meV/atom represent only a fraction of the interlayer interaction E_{il}. Since the interlayer distances are large and interlayer interactions are small in all four phases, the optimized layer structures of the bulk system and the monolayer are nearly indistinguishable. The fact that the interlayer interaction is

TABLE I.   Observed and calculated properties of the four layered bulk phosphorus allotropes. $|\vec{a_1}|$ and $|\vec{a_2}|$ are the in-plane lattice constants defined in Fig. 1. d is the interlayer separation, and E_{il} is the interlayer separation energy per atom. E_{coh} is the cohesive energy with respect to isolated atoms. $\Delta E_{coh} = E_{coh} - E_{coh}$ (α-P) is the relative stability of the layered allotropes with respect to the most stable black phosphorene (or α-P) phase.

Phase	α-P (exp.)	α-P (theory)	β-P (theory)	γ-P (theory)	δ-P (theory)
$|\vec{a_1}|$ (Å)	4.38[a]	4.53[b]	3.33[b]	3.41[b]	5.56[b]
$|\vec{a_2}|$ (Å)	3.31[a]	3.36[b]	3.33[b]	5.34[b]	5.46[b]
d (Å)	5.25[a]	5.55[b]	5.63[b]	4.24[b]	5.78[b]
	$\cdots$	5.30[c]	4.20[c]	4.21[c]	5.47[c]
E_{il} (eV/atom)	$\cdots$	0.02[b]	0.01[b]	0.03[b]	0.02[b]
	$\cdots$	0.12[c]	0.10[c]	0.13[c]	0.11[c]
E_{coh} (eV/atom)	3.43[d]	3.30[b]	3.29[b]	3.22[b]	3.23[b]
ΔE_{coh} (eV/atom)	$\cdots$	0.00[b]	−0.01[b]	−0.08[b]	−0.07[b]
	$\cdots$	0.00[c]	−0.04[c]	−0.09[c]	−0.08[c]

[a]Experimental data of Ref. [19].
[b]Results based on the DFT-PBE functional [12] with a spin-polarized P atom as a reference [20].
[c]Results based on the optB86b van der Waals functional [17,18].
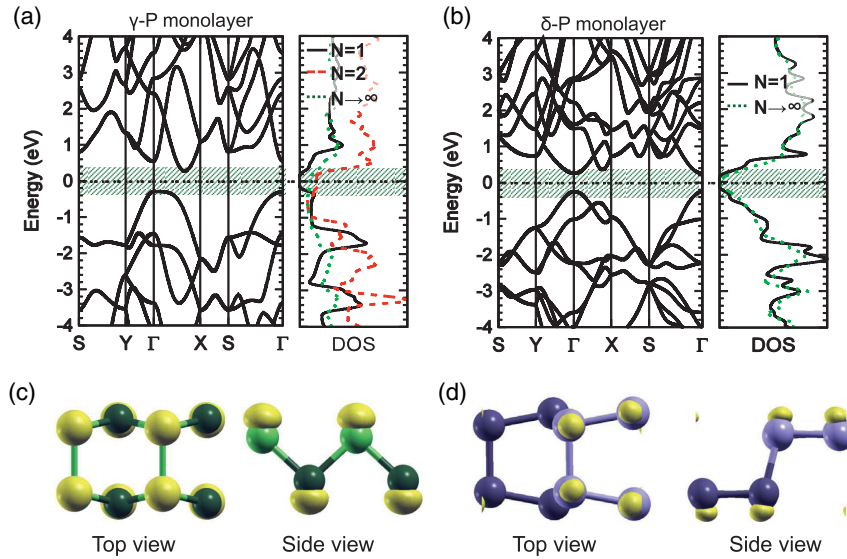[d]Experimental value for bulk phosphorus [21].

FIG. 2 (color online).   Electronic band structure and density of states (DOS) of (a) γ-P and (b) δ-P monolayers. Results for bilayer and bulk systems are shown for comparison in the DOS plots only. Top and side views of the electron density ρ_{vc} near the top of the valence and the bottom of the conduction bands of (c) γ-P and (d) δ-P. Only states in the energy range $E_F - 0.4$ eV $< E < E_F + 0.4$ eV are considered, as indicated by the green shaded region in (a) and (b). ρ_{vc} is represented at the isosurface value $\rho_{vc} = 1.1 \times 10^{-3}$ e/Å^3 for γ-P and δ-P and superposed with a ball-and-stick model of the structure.

similarly small in all phases indicates the possibility of layer-by-layer exfoliation not only of black phosphorus [4], but also the other layered allotropes.

We present results of our DFT-PBE electronic band structure calculations for γ-P and δ-P monolayers in Fig. 2. As can also be inferred from the numerical results in the related Table II, the fundamental band gaps in γ-P and δ-P are somewhat smaller than those of α-P and β-P monolayers, but still significant. Since our *GW* self-energy calculations indicate that these DFT-PBE band-gap values are underestimated by ≈ 1 eV, as expected for DFT calculations, all four phases should display a fundamental band gap in excess of 1 eV in the monolayer. Whereas γ-P has an indirect band gap, δ-P is a direct band-gap semiconductor. Besides the electronic band structure of the monolayers, we present the associated density of states of a monolayer and of the bulk system in Figs. 2(a) and 2(b). As already noticed for the α-P and β-P structures [4,6], the electronic structure near E_F including the band gap depends sensitively on the number of layers in all phosphorene allotropes, including γ-P and δ-P. The most noted difference in the density of states of γ-P in Fig. 2(a) is between a semiconductor for $N = 1$ and a metal for $N \geq 2$.

Whereas DFT calculations typically underestimate the fundamental band gap, they are believed to correctly represent the electronic structure in the valence and the conduction band region. To get a better impression about the nature of conducting states in doped γ-P and δ-P, we display the charge distribution associated with states near the Fermi level in Figs. 2(c) and 2(d), superposed with the atomic structure. These states and their hybrids with

electronic states of the contact electrodes will play a crucial role in the carrier injection and quantum transport. We find these conduction states to have the character of p states normal to the layers, similar to graphene. In multilayer systems, these states hybridize between adjacent layers, causing a band dispersion normal to the slab. This causes a change in the density of states in the gap region between a monolayer and the bulk structure.

To judge how the fundamental band gap depends on the slab thickness, we present our DFT-PBE band-gap results for α-P, β-P, γ-P, and δ-P as a function of the number of layers N in Fig. 3(a). Our most important finding is that the band gap vanishes for $N \geq 2$ in γ-P, turning bilayers and thicker slabs metallic.

A similarly intriguing picture emerges when studying the dependence of the fundamental band gap on the in-layer strain. Results for strain applied in two orthogonal directions are shown in Fig. 3(b) for γ-P and in Fig. 3(c) for δ-P. Again, our most significant finding is that stretching beyond 4% should turn a γ-P monolayer metallic.

As already reported for α-P and β-P [4,6–8], applying even a relatively low level of in-layer strain causes drastic changes in the band gap and may even change its character from direct to indirect. The latter fact is a consequence of

TABLE II.   The fundamental band gap E_g in monolayers of α-P, β-P, γ-P, and δ-P, based on DFT-PBE calculations.

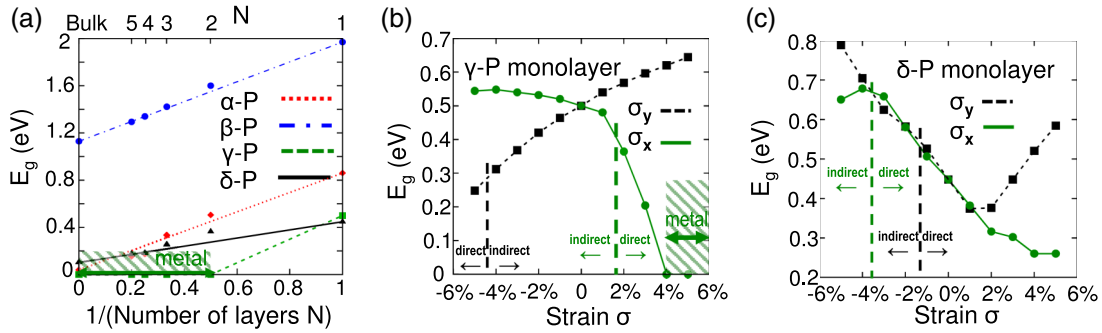| Phase	α-P	β-P	γ-P	δ-P
E_g (eV)	0.90	1.98	0.50	0.45

FIG. 3 (color online).   (a) Dependence of the fundamental band gap E_g on the slab thickness in N-layer slabs of α-P (black), β-P (blue), γ-P, and δ-P. Dependence of the fundamental band gap on in-layer strain is presented in (b) for γ-P and in (c) for δ-P. The strain direction is defined in Fig. 1. The shaded regions in (a) and (b) highlight conditions under which γ-P becomes metallic. Dashed vertical lines in (b) and (c) indicate a direct-to-indirect band-gap transition.

several valleys in the conduction band, which may change their relative depth due to lattice distortions. Strain of up to a few percent may be accomplished when phosphorene is grown epitaxially on a particular substrate. We may even consider the possibility of in-layer band-gap engineering by substrate patterning.

Even richer possibilities for band structure engineering should arise by in-layer connections between the different phases. In-layer connections, which have been observed in hybrid systems of graphene and hexagonal BN [27], suffer from large interface energy penalties due to the lack of commensurability. The situation is very different in phosphorene, since the four layered allotropes share the same structural motif of threefold-coordinated P atoms surrounded by nearest neighbors in a tetrahedral arrangement. We find that this tetrahedral arrangement can be maintained even within specific in-layer connections of the different structures, resulting in an extremely low energy penalty.

We have optimized the structure of in-layer connections between α-P and β-P, between β-P and γ-P, and between γ-P and δ-P. Our results, depicted in Fig. 4, indicate that an optimum connection involves different orientations of the joined planes. The optimization calculations, performed in

supercell geometry with varying cell sizes, allowed us to determine the energy cost per edge length $\Delta E_c/l$ to connect two structural phases. To obtain this quantity for a connection between phases 1 and 2, we considered N_1 atoms of phase 1 and N_2 atoms of phase 2 per unit cell and varied the N_1/N_2 ratio while keeping the same length of the interface boundary. For a reliable estimate of the energy penalty associated with forming an interface between the two phases, we compared total energies of optimized structures with coexisting phases to those of pure, defect-free phases. Our results for $\Delta E_c/l$ for the connections shown in Fig. 4 are listed in Table III, along with the optimum values of the connection angle φ.

The energy results in Table III indicate that the energy cost to connect stable but different structural phases is negligible in comparison to the cohesive energy. The implication that coexistence of several phases within one layer is not energetically penalized is extremely uncommon in nature. We can envisage the possibility of forming such multiphase structures by depositing phosphorene monolayers on a substrate with a specific step structure, such as a vicinal surface, using chemical vapor deposition. The domain wall boundaries between different phases
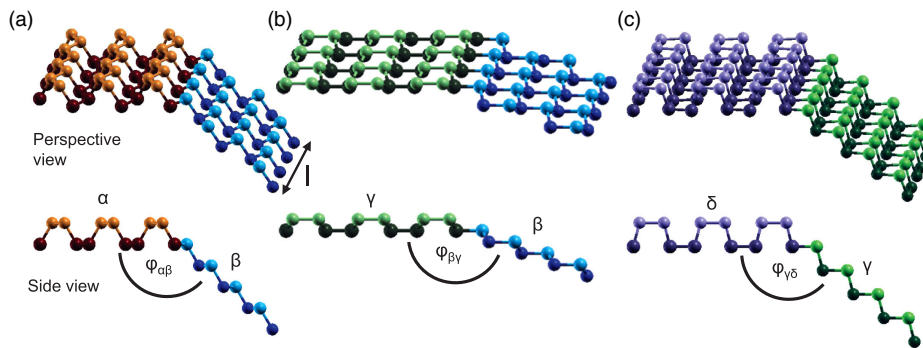

FIG. 4 (color online).   Energetically favorable in-layer connections between (a) α-P and β-P, (b) β-P and γ-P, and (c) γ-P and δ-P, shown in perspective and side view. l represents the edge length at the interface, and φ is the connection angle. The color scheme for the different allotropes is the same as in Fig. 1.

TABLE III.   Energy cost per edge length $\Delta E_c/l$ and connection angle φ, defined in Fig. 4, associated with connecting two semi-infinite phosphorene monolayers.

Phase connection	α-β	β-γ	γ-δ
$\Delta E_c/l$	< 1 meV/Å	< 17 meV/Å	< 6 meV/Å
Angle φ	142°	160°	145°

may also move to optimize adhesion to an inhomogeneous or nonplanar substrate. The electronic properties of a heterostructure within one layer will depend on not only the electronic structure of the pure phases, but also their finite width or size and the defect bands associated with the interfaces. In principle, it should be possible to form a complex device structure by a judicious arrangement of different structural phases within one phosphorene monolayer.

Monolayers containing the four layered phosphorene phases are expected to be not only stable, but also flexible. Consequently, the nonplanarity of multiphase structures does not pose a real problem. It may even provide the advantage to form complex foam structures, similar to graphitic carbon foams, with unusual electronic properties [28,29].

In conclusion, based on *ab initio* density functional calculations, we have proposed γ-P and δ-P as two additional stable structural phases of layered phosphorus besides the layered α-P (black) and β-P (blue) phosphorus allotropes. Monolayers of some of these allotropes have a wide band gap, whereas others, including γ-P, show a metal-insulator transition caused by in-layer strain or changing the number of layers. An unforeseen benefit is the possibility to connect different structural phases at no energy cost. This becomes particularly valuable in assembling heterostructures with well-defined metallic and semiconducting regions in one contiguous layer.

---

[*]tomanek@pa.msu.edu

[1] S. Narita, Y. Akahama, Y. Tsukiyama, K. Muro, S. Mori, S. Endo, M. Taniguchi, M. Seki, S. Suga, A. Mikuni, and H. Kanzaki, Physica (Amsterdam) **117–118**, 422 (1983).

[2] Y. Maruyama, S. Suzuki, K. Kobayashi, and S. Tanuma, Physica (Amsterdam) **105B+C**, 99 (1981).

[3] L. Li, Y. Yu, G. J. Ye, Q. Ge, X. Ou, H. Wu, D. Feng, X. H. Chen, and Y. Zhang, Nat. Nanotechnol. **9**, 372 (2014).

[4] H. Liu, A. T. Neal, Z. Zhu, Z. Luo, X. Xu, D. Tomanek, and P. D. Ye, ACS Nano **8**, 4033 (2014).

[5] S. P. Koenig, R. A. Doganov, H. Schmidt, A. H. Castro Neto, and B. Özyilmaz, Appl. Phys. Lett. **104**, 103106 (2014).

[6] Z. Zhu and D. Tománek, Phys. Rev. Lett. **112**, 176802 (2014).

[7] A. S. Rodin, A. Carvalho, and A. H. Castro Neto, Phys. Rev. Lett. **112**, 176801 (2014).

[8] R. Fei and L. Yang, Nano Lett. **14**, 2884 (2014).

[9] J. C. Jamieson, Science **139**, 1291 (1963).

[10] S. E. Boulfelfel, G. Seifert, Y. Grin, and S. Leoni, Phys. Rev. B **85**, 014110 (2012).

[11] E. Artacho, E. Anglada, O. Dieguez, J. D. Gale, A. Garcia, J. Junquera, R. M. Martin, P. Ordejon, J. M. Pruneda, D. Sanchez-Portal, and J. M. Soler, J. Phys. Condens. Matter **20**, 064208 (2008).

[12] J. P. Perdew, K. Burke, and M. Ernzerhof, Phys. Rev. Lett. **77**, 3865 (1996).

[13] N. Troullier and J. L. Martins, Phys. Rev. B **43**, 1993 (1991).

[14] H. J. Monkhorst and J. D. Pack, Phys. Rev. B **13**, 5188 (1976).

[15] M. R. Hestenes and E. Stiefel, J. Res. Natl. Bur. Stand. **49**, 409 (1952).

[16] G. Kresse and J. Furthmüller, Phys. Rev. B **54**, 11169 (1996).

[17] J. Klimeš, D. R. Bowler, and A. Michaelides, J. Phys. Condens. Matter **22**, 022201 (2010).

[18] J. Klimeš, D. R. Bowler, and A. Michaelides, Phys. Rev. B **83**, 195131 (2011).

[19] R. Hultgren, N. S. Gingrich, and B. E. Warren, J. Chem. Phys. **3**, 351 (1935).

[20] The spin polarization energy of an isolated P atom is 1.91 eV in PBE. Ignoring spin polarization of the P atom reference would increase the cohesive energy by this amount.

[21] C. Kittel, *Introduction to Solid State Physics*, 8th ed. (Wiley, Hoboken, NJ, 2004).

[22] See Supplemental Material at http://link.aps.org/supplemental/10.1103/PhysRevLett.113.046804 for molecular dynamics simulations and phonon spectra of γ-P and δ-P monolayers.

[23] V. V. Gobre and A. Tkatchenko, Nat. Commun. **4**, 2341 (2013).

[24] W. Gao and A. Tkatchenko, Phys. Rev. Lett. **111**, 045501 (2013).

[25] L. Shulenburger and T. R. Mattsson, Phys. Rev. B **88**, 245117 (2013).

[26] L. Shulenburger (private communication).

[27] Z. Liu, L. Ma, G. Shi, W. Zhou, Y. Gong, S. Lei, X. Yang, J. Zhang, J. Yu, K. P. Hackenberg, A. Babakhani, J.-C. Idrobo, R. Vajtai, J. Lou, and P. M. Ajayan, Nat. Nanotechnol. **8**, 119 (2013).

[28] Z. Zhu and D. Tománek, Phys. Rev. Lett. **109**, 135501 (2012).

[29] Z. Zhu, Z. G. Fthenakis, J. Guan, and D. Tománek, Phys. Rev. Lett. **112**, 026803 (2014).